

RESEARCH ARTICLE

Alteration of the $\alpha_1\beta_2/\alpha_2\beta_1$ subunit interface contributes to the increased hemoglobin-oxygen affinity of high-altitude deer mice

Noriko Inoguchi¹, Nobuhiro Mizuno², Seiki Baba², Takashi Kumasaka², Chandrasekhar Natarajan¹, Jay F. Storz¹, Hideaki Moriyama^{1*}

1 School of Biological Sciences, University of Nebraska, Lincoln, Nebraska, United States of America, **2** Protein Crystal Analysis Division, Japan Synchrotron Radiation Research Institute, Sayo, Japan

* hideaki@unl.edu



Abstract

Background

Deer mice (*Peromyscus maniculatus*) that are native to high altitudes in the Rocky Mountains have evolved hemoglobins with an increased oxygen-binding affinity relative to those of lowland conspecifics. To elucidate the molecular mechanisms responsible for the evolved increase in hemoglobin-oxygen affinity, the crystal structure of the highland hemoglobin variant was solved and compared with the previously reported structure for the lowland variant.

Results

Highland hemoglobin yielded at least two crystal types, in which the longest axes were 507 and 230 Å. Using the smaller unit cell crystal, the structure was solved at 2.2 Å resolution. The asymmetric unit contained two tetrameric hemoglobin molecules.

Conclusions

The analyses revealed that α Pro50 in the highland hemoglobin variant promoted a stable interaction between α His45 and heme that was not seen in the α His50 lowland variant. The α Pro50 mutation also altered the nature of atomic contacts at the $\alpha_1\beta_2/\alpha_2\beta_1$ intersubunit interfaces. These results demonstrate how affinity-altering changes in intersubunit interactions can be produced by mutations at structurally remote sites.

Introduction

Hemoglobin is a heterotetrameric protein consisting of two α subunits and two β subunits, and each subunit has an iron-centered heme that reversibly binds oxygen [1]. Hemoglobin transports heme-bound oxygen from the lungs to all of the tissues in the body via oxygenation-linked shifts in the conformational equilibrium between the tense state (T state; deoxygenated) and the relaxed state (R state; oxygenated) [1–3]. This structural transition is controlled allosterically, as the binding of oxygen to one subunit affects the oxygen-affinity of

OPEN ACCESS

Citation: Inoguchi N, Mizuno N, Baba S, Kumasaka T, Natarajan C, Storz JF, et al. (2017) Alteration of the $\alpha_1\beta_2/\alpha_2\beta_1$ subunit interface contributes to the increased hemoglobin-oxygen affinity of high-altitude deer mice. PLoS ONE 12(3): e0174921. <https://doi.org/10.1371/journal.pone.0174921>

Editor: Eugene A. Permyakov, Russian Academy of Medical Sciences, RUSSIAN FEDERATION

Received: January 8, 2017

Accepted: March 17, 2017

Published: March 31, 2017

Copyright: © 2017 Inoguchi et al. This is an open access article distributed under the terms of the [Creative Commons Attribution License](https://creativecommons.org/licenses/by/4.0/), which permits unrestricted use, distribution, and reproduction in any medium, provided the original author and source are credited.

Data Availability Statement: The structure was deposited in the Protein Data Bank with the ID code 5KER.

Funding: National Institute of Health/National Heart, Lung, and Blood Institute (HL087216). University of Nebraska.

Competing interests: The authors have declared that no competing interests exist.

the other subunits in the same tetrameric assembly [3]. Therefore, studies of structure-function relationships in hemoglobin have focused on heme-ligand binding at the active site [4, 5] as well as the oxygenation-linked conformational changes between the R and the T states [6–8]. Recent studies suggest the presence of several intermediate states between structural transitions [9–11].

When air-breathing vertebrates are exposed to environmental hypoxia, an increase in hemoglobin-oxygen affinity can compensate for the reduced partial pressure of oxygen in inspired air by safeguarding arterial oxygen saturation [12–14]. To investigate the structural basis of evolved changes in hemoglobin-oxygen affinity, we chose to focus on functionally well-characterized hemoglobin variants of the deer mouse, *Peromyscus maniculatus*. Populations of deer mice that are native to high-altitudes in the Rocky Mountains have evolved a genetically based increase in hemoglobin-oxygen affinity relative to lowland conspecifics in the prairie grassland. The hemoglobin of the highland mice has a higher intrinsic oxygen-affinity, and this affinity difference is further accentuated in the presence of chloride ions and 2,3-diphosphoglycerate (DPG) [15–19]. The most common hemoglobin variants of high- and low-altitude deer mice are distinguished by a total of 12 amino acid substitutions—eight in the α subunit and four in the β subunit (Fig 1A). The oxygenation properties of these alternative variants are well-characterized [15–19], but the structural basis of the observed differences in oxygen affinity has not been fully elucidated.

Previously, we solved the 3D structure of the lowland hemoglobin variant of deer mice (PDB ID: 4H2L), and structural comparisons with human hemoglobin showed that α His45 is oriented toward the solvent in this lowland variant, whereas α His45 in human hemoglobin interacts with heme [20]. This unique α His45 configuration was also observed in horse hemoglobin crystallized with 2-[4-(3,5-dichlorophenylureido) phenoxy]-2-methylpropionic acid (L35) (PDB ID: 2D5X) [21].

We solved the crystal structure of the highland hemoglobin variant to gain further structural insights into the molecular mechanism responsible for the evolved increase in oxygen-binding affinity. A comparative analysis of the highland and lowland deer mouse hemoglobin variants revealed that main chain displacements were present between α 41 and α 54, the loop region near heme, which resulted from a α 50His \rightarrow Pro mutation in the highland variant. The difference was also highlighted by the interaction between α His45 and heme in the highland hemoglobin variant. In addition, the highland hemoglobin variant had a reduced intersubunit contact surface, particularly at the $\alpha_1\beta_2/\alpha_2\beta_1$ switch region.

These analyses suggest that the loose intersubunit interfaces in the highland hemoglobin molecule confers a flexible structure that shifts the allosteric equilibrium towards the R state by lowering the free energy of the R \leftrightarrow T transition, thereby increasing oxygen affinity.

Materials and methods

This study was carried out in accordance with the recommendations in the Guidelines-Research involving Recombinant or Synthetic Nucleic Acid Molecules of the National Institutes of Health. The protocol was approved by the Institutional Biosafety Committee of the University of Nebraska-Lincoln (Protocol ID: 174).

Purification and crystallization of recombinant highland hemoglobin

Recombinant highland deer mouse hemoglobin in the carbon monoxide format was produced as previously described [20, 22]. Purified highland hemoglobin was crystallized with the vapor diffusion method using 26% (w/v) PEG 3350 in 50 mM sodium/potassium phosphate buffer, pH 8.0, at 299 K in the airtight vial purged with carbon monoxide (S1 Fig). We dissolved the

α subunit

	10	20	30	40	50
Deer mouse (H)	VLSADDKANI	KAAWGKIGGH	GAEYGAEALE	RMFCSFPTTK	TYPPHFDVSP
Deer mouse (L)H
Human	...PA...TVV.A.	AG.....LLL

	60	70	80	90	100
Deer mouse (H)	GSAQVKHGGA	KVAGALATAA	SHLDDLPAAL	SALSDLHAHK	LRVDPVNFKL
Deer mouse (L)A.GDG
HumanG.KTN.V	A.V..M.N

	110	120	130	140
Deer mouse (H)	LSHCLLVTLA	AHHPAEFTPA	VHASLDRKFLA	SVSTVLTSKY R
Deer mouse (L)L.SD
HumanAE

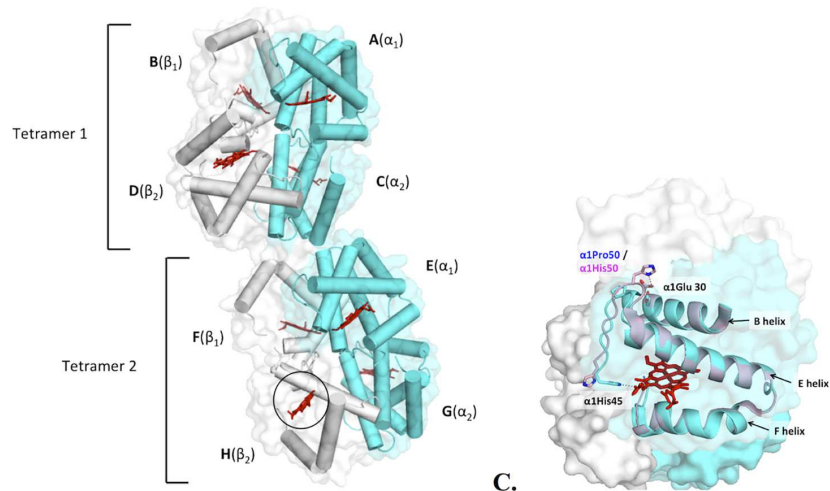
β subunit

	10	20	30	40	50
Deer mouse (H)	VHLTDAEKAL	VTGLWGKVP	EEIGGEALGR	LLAVYPWTQR	FFDSFGDLSS
Deer mouse (L)
Human	...PE..SA	..A....NV	D.V.....	..V.....	..E.....T

	60	70	80	90	100
Deer mouse (H)	ASAIMGNKV	KGHGKVIDS	FGEGLKHLND	LKGTFAISLE	LHCCKLHVDP
Deer mouse (L)ASS
Human	PD.V...P	..A....LGA	.SD..A....T

	110	120	130	140
Deer mouse (H)	ENFKLLGNMI	VIVMAHHLGK	DFTPAQAAY	QKVVAGVATA LAHKYH
Deer mouse (L)SS
Human	...R...VL	.C.L...F	E...PV.SN

A.



B.

C.

Fig 1. Sequence comparisons and differences in the α subunit main chain coordinates between highland and lowland hemoglobin. (A) Sequence alignment of deer mouse highland (H) and lowland (L) hemoglobin. The substitutions are highlighted in blue. The sequences were obtained from the deposited structures as follows: highland deer mouse hemoglobin (PDB ID: 5KER), lowland deer mouse hemoglobin (4H2L), human hemoglobin (2DN1). (B) Orientation of two tetrameric hemoglobin molecules in an asymmetric unit. The α subunits are colored in cyan, and the β subunits are colored in gray. Heme in each subunit is shown as a red stick model, and the active site without ligand assignment is indicated with a black circle. (C) Structural difference in main chain folding with an emphasis on αHis45 coordinates. Tetrameric highland hemoglobin (5KER; cyan) and lowland hemoglobin (4H2L, pink) are superimposed by PyMOL. The residues around the active site and the nearby loop region are shown in the cartoon model. Key residues and helices containing these residues in the α subunit (chain A) are shown in the stick model and the cartoon model.

<https://doi.org/10.1371/journal.pone.0174921.g001>

crystals 65 days after they were formed, and UV-visible spectroscopy revealed the spectrum expected for carboxy hemoglobin. Diffractable crystals were obtained in fiber clusters with 5 mM glutathione, 0.1% (v/v) 2,4-pentanediol and 7 mM calcium chloride (S1 Fig). The lowland hemoglobin variant was crystallized under the same conditions as the highland variant with the exception that 28% (w/v) PEG 3350 was used; however, the same fibrous format was not observed. Crystals of lowland hemoglobin were produced only with 14 mM calcium chloride without glutathione and 2,4-pentanediol [20].

Preliminary X-ray diffraction analysis

At least two types of crystals were grown. However, in both cases, the crystals were fragile and had a high mosaic spread in the diffraction images. Multiple attempts were required to obtain an interpretable diffraction image by HKL2000 (HKL Research, Charlottesville, VA, USA) [23]. The first crystal (type F) was subjected to the diffraction experiment at BL41XU at the SPring-8. The type F crystal diffracted up to a 3.0 Å resolution, and the crystal belonged to the space group $C222/C222_1$ with the unit cell dimensions $a = 53$, $b = 91$ and $c = 507$ Å. The second crystal (type S) was analyzed at the 14-BM-C, BioCARS of the Advanced Photon Source (APS) at Argonne National Laboratory. The type S crystal diffracted beyond 2.2 Å resolution and belonged to the space group $P2_1$ with the unit cell dimensions $a = 53.18$, $b = 229.62$, $c = 53.29$ Å and $\beta = 119.12^\circ$ (Table 1). Considering the compactness of the unit cell, we solved the structure of highland hemoglobin using the type S crystal.

Table 1. Data collection and refinement statistics of the type S crystal.

Data collection	
Wavelength (Å)	0.978
Resolution range (Å)	29.56–2.202 (2.281–2.202)
Space group	$P2_1$
Unit cell (Å, °)	53.18 229.62 53.29, 90 119.12 90
Total reflections	65478 (4715)
Unique reflections	39866 (3273)
Multiplicity	1.6 (1.4)
Completeness (%)	0.71 (0.59)
Mean $I/\sigma(I)$	9.26 (3.49)
Wilson B-factor	22.28
R-merge	0.08958 (0.2582)
$CC_{1/2}$	0.983 (0.665)
Refinement	
R-work	0.1931 (0.3292)
R-free	0.2017 (0.3579)
CC (work)	0.952 (0.635)
CC (free)	0.949 (0.597)
macromolecules	8604
ligands	344
protein residues	1144
RMS (bonds)	0.007
RMS (angles)	1.12
Ramachandran favored (%)	96
Ramachandran allowed (%)	3.5
Ramachandran outliers (%)	0
Rotamer outliers (%)	1.2
Clashscore	7.24
Average B-factor	28.98
macromolecules	28.87
ligands	27.00
solvent	31.33

Statistics for the highest-resolution shell are shown in parentheses.

<https://doi.org/10.1371/journal.pone.0174921.t001>

Data collection and structure refinement

The diffraction data for the type S crystal were collected from a flash frozen single crystal under the cold stream at 90 K using 10% (v/v) glycerol as the cryo-protectant. Diffraction images were recorded by the ADSC Q315 detector at the 14-BM-C using the X-ray wavelength 0.978 Å at 14-B-C, APS BioCARS. We used the oscillation method with a swing width of 1°. We collected two data sets to cover 180° of the spindle for each using κ angles of 0° and 30°. During data collection, the crystal suffered immense radiation damage. After iterative image data processing using HKL2000 [23], only the first dataset with $\kappa = 0^\circ$ was usable, in which only 128 images out of 180 images were interpreted. The collected diffraction data exhibited anisotropy, limiting data collection beyond 3.0 Å resolution along the L-axis. This resulted in 71% completeness, but we were still able to achieve a higher signal to noise ratio ($I/\sigma > 9$) and a resolution up to 2.2 Å (Table 1). Despite the weak diffraction data statistics, we proceeded to the structure analysis, taking advantage of the consistent folding of hemoglobin. The phase was recovered using the molecular replacement method with lowland deer mouse hemoglobin as the search model (PDB ID: 4H2L) in Phenix [24]. The obtained solution was manually fitted to the electron density using Coot [25] and was then further refined by running phenix.refine. The fitting between the electron density map and the model was good. However, the last residue in all of the α chains, α 141Arg, was not assigned in the final model because of weak electron density. The crystallographic statistics are listed in Table 1. The structure was deposited in the Protein Data Bank with the ID code 5KER. The obtained highland hemoglobin structure had two heterotetrameric hemoglobin molecules in the asymmetric unit. The chain ID allocations in this PDB entry were as follows: one tetramer consisted of chains A (α_1), B (β_1), C (α_2) and D (β_2), and the other of chains E, F, G and H in the same order. PyMOL (Version 1.8 Schrödinger, LLC.) was used for structural mining.

Results

Structure of the highland hemoglobin variant

The type S highland hemoglobin crystal contained 2 tetramers in the asymmetric unit (Fig 1B) that were connected by intersubunit hydrogen bonds between subunits C, D, E and F (Table 2). Although the UV-visible spectrum of the dissolved crystal solution indicated the presence of carboxyhemoglobin, we were only able to assign a water molecule at each heme based on the obtained electron density map. In addition, chain H (β subunit), did not have an assigned ligand, as there was no electron density supporting the presence of a molecule of carbon monoxide, oxygen, or water (S2 Fig). Lowland hemoglobin was also in water-bound form, but it had one α and one β subunit in the asymmetric unit [20], as is often observed in liganded tetrameric hemoglobin structures including human hemoglobin [26].

At the tetramer interface, chain F and C had the highest subunit interaction area. One of the identified hydrogen bonds between α_1 C-Ala115 (N) and β_1 F-Asp121 (OD1) could be unique, as the lowland hemoglobin variant has Ser at α 115. However, none of the identified interactions was located near the distal heme pocket. The two tetramers folded similarly with

Table 2. Interacting amino acids of the 2 tetramers.

Subunit interaction (area)	Interaction	Distance
Chain C/E (113.2 Å ²)	α_1 C-Lys16 (NZ): α_1 E-Ala111 (O)	3.21 Å
Chain C/F (232.2 Å ²)	α_1 C-His20 (NE2): β_1 F-His117 (O)	3.56 Å
	α_1 C-Ala115 (N): β_1 F-Asp121 (OD1)	3.07 Å
Chain D/F (56.1 Å ²)	β_2 D-Lys120 (NZ): β_1 F-Gly16 (O)	2.32 Å

<https://doi.org/10.1371/journal.pone.0174921.t002>

an r.m.s. value of 0.54 between ABCD and EFGH according to the PyMOL alignment function. Of note, in the sickle-cell deoxyhemoglobin (deoxyHbS) fiber using the same chain designation as the present structure, the head to tail tetramer interactions were α_1 C-Pro114: β_1 F-Glu121 [27]. The interactions observed during polymerization were different between deoxyHbS and the present structure.

Main chain traces between each subunit of the highland and lowland hemoglobin variants were highly similar, with r.m.s.d. values falling within 0.3–0.8 Å, except for the terminal residues using the CCP4 superposing program [28]. Higher displacements in the main chain atoms were found in the α subunit residues between 41 and 54 with r.m.s.d. values of 1.2–2.6 Å. This was caused by the amino acid mutation at position α 50 (Fig 1C; see the following section). β subunit main chain traces between highland and lowland hemoglobin showed no detectable displacements.

Effects of the α 50 mutation on the configuration of α His45 and the $\alpha_1\beta_2/\alpha_2\beta_1$ switch interface

Among the 12 amino acid mutations that distinguish the lowland and highland hemoglobin variants, one especially noteworthy change involved the replacement of α Pro50 in highland hemoglobin for α His50 in lowland hemoglobin (Fig 1A and 1C). Based on the main chain atom displacements, this α His50Pro mutation changed the coordinates of the nearby loop region as well as that of α His45. The α 50 and α His45 residues are located in the loop region leading to the E helix, and this loop is relatively rigid because it is stabilized by hydrogen bonds according to the Dictionary of Secondary Structure of Proteins (DSSP) [29, 30] (data not shown). In the lowland hemoglobin variant, α His50 interacts with α Glu30 (Fig 1C, [19]), which pinches the amino end of the loop and prevents a stable α His45-heme interaction. This resulted in α His45 interacting with nearby residues in the crystal symmetry relationship [20]. In the highland hemoglobin variant, this pinching was not observed because α Pro50 has no interaction with α Glu30. As a result, the highland hemoglobin variant could have a stable α His45-heme interaction. In fish hydrated hemoglobin, the contribution of α His45 in heme retention reported [31], which supports our assumptions.

The difference in the loop region also affected intersubunit interactions. Hemoglobin exhibits allosteric motion in the transition between the T and R states, and this oxygenation-linked transition alters a set of subunit contacts at the $\alpha_1\beta_2/\alpha_2\beta_1$ switching region (Fig 2). In human hemoglobin, the highlighted residues at this switching region are Thr38, Thr41 and Pro44 from the α_1/α_2 subunit C/D helix and His97 from the β_2/β_1 subunit [32, 33]. In deoxygenated hemoglobin (T), β_2 His97 is located close to α_1 Pro44, whereas in oxygenated hemoglobin (R), β_2 His97 faces away from α_1 Pro44 [10, 32, 33]. In the case of deer mouse hemoglobin (Fig 1A), both highland and lowland hemoglobin variants have the same amino acid residues at the switch region as the case of human hemoglobin. Although the superimposed structure showed that the distance between α_1 Thr38 C_α from highland and lowland hemoglobin was within a 0.3 Å difference, the distance comparisons between the α_1 Thr41 pairs and α_1 Pro44 pairs increased to 1.1 Å and 1.4 Å, respectively (Fig 2). In addition, the distance between α_1 Thr38, α_1 Thr41 and α_1 Pro44 with respect to β_2 His97 was shorter in the lowland hemoglobin variant than in the highland variant (Table 3).

Although the C_α coordinates of residues at each switching region from highland hemoglobin were the same, the relative orientation of the β_2 His97 imidazole ring was different, particularly at chain G and F ($\alpha_2\beta_1$ interface, Fig 2).

Comparisons of subunit interfaces between the highland and lowland hemoglobin variants using the PISA webserver [34] showed other differences in the $\alpha_1\beta_2/\alpha_2\beta_1$ interface interactions.

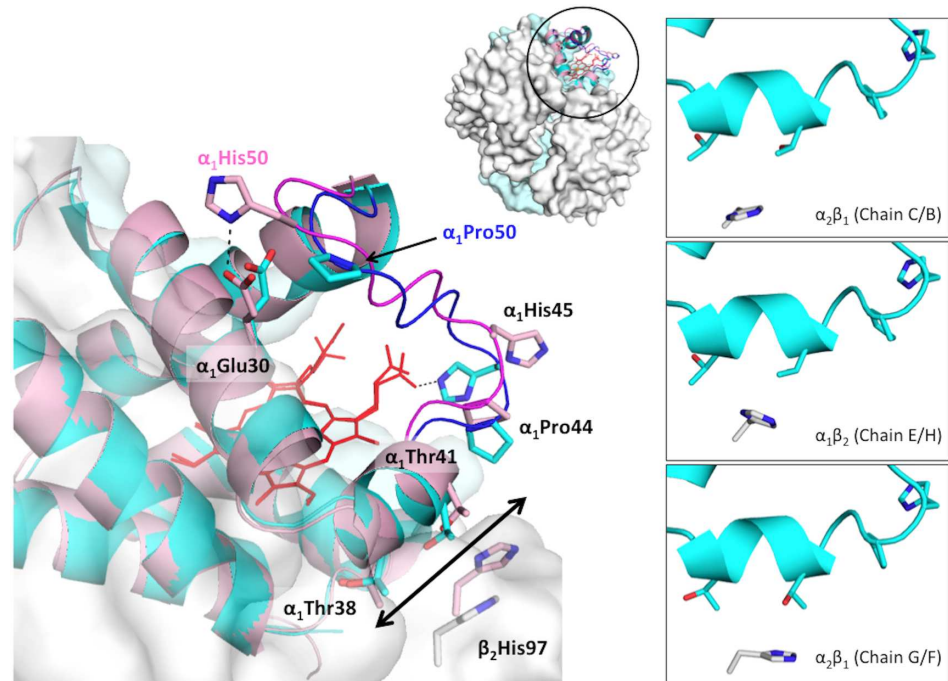


Fig 2. Difference in the $\alpha_1\beta_2$ switching region interaction between highland and lowland hemoglobin. The α subunit is shown in the cartoon, and the key residues are represented as a stick model. The residues unique to highland and lowland hemoglobin are labeled in cyan and pink, respectively. The highland hemoglobin α_1 subunit is colored in cyan, and its β_2 subunit is colored in gray. Both subunits from the lowland hemoglobin are colored in pink. The right side boxes indicate differences in the $\alpha_1\beta_2/\alpha_2\beta_1$ interface coordinates, particularly the β_2 His 97 imidazole ring orientation relative to the α_1 residues.

<https://doi.org/10.1371/journal.pone.0174921.g002>

For example, the interaction between α_1 Arg92 and β_2 Asp43 was different due to the change in the orientation of α_1 Arg92. This particular interaction was not observed between chains G (α subunit) and F (β subunit) (Fig 3) in highland hemoglobin. Nevertheless, the α_1 Arg92 / β_2 Asp43 interaction was found in chain H, the subunit without assigned ligand (Fig 1B and S2 Fig) Since chain H had a planar heme like a typical in liganded hemoglobin, alterations of $\alpha_1\beta_2/\alpha_2\beta_1$ interface appear to affect hemoglobin-oxygen affinity.

In addition, highland hemoglobin has a reduced subunit contact surface at the $\alpha_1\beta_2/\alpha_2\beta_1$ interface, and this difference in interface area between the lowland and highland hemoglobin variants is similar in magnitude to the difference between oxygenated and deoxygenated states of human hemoglobin (Fig 4). In particular, lowland hemoglobin has about 30% larger $\alpha_1\beta_2/\alpha_2\beta_1$ interface that is expected for the T-state [20]. Just as the T-state quaternary structure has lower oxygen-binding affinity than the R-state quaternary structure [35, 36], the highland hemoglobin variant has a higher oxygen-binding affinity than lowland hemoglobin variant.

Table 3. C_α distances at $\alpha_1\beta_2/\alpha_2\beta_1$ switching region.

Hemoglobin	Interface (chains)	α_1 Thr38: β_2 His 97	α_1 Thr41: β_2 His 97	α_1 Pro44: β_2 His 97
Lowland	$\alpha_1\beta_2$ (A/D)	5.0 Å	7.3 Å	12.2 Å
Highland	$\alpha_1\beta_2$ (A/D)	6.7 Å	8.7 Å	13.9 Å
	$\alpha_2\beta_1$ (C/B)	6.7 Å	8.7 Å	13.7 Å
	$\alpha_1\beta_2$ (E/H)	6.0 Å	7.7 Å	12.9 Å
	$\alpha_2\beta_1$ (G/F)	6.5 Å	8.3 Å	13.3 Å

<https://doi.org/10.1371/journal.pone.0174921.t003>

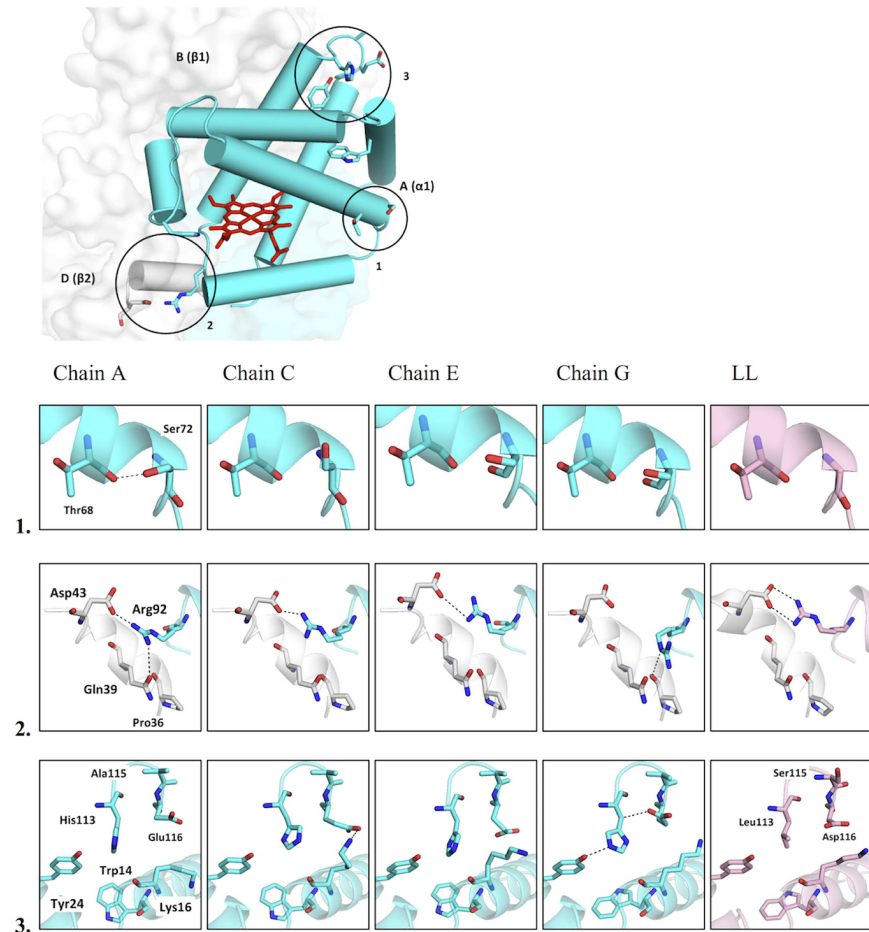


Fig 3. Unique interactions present in highland hemoglobin. Locations of unique interactions. Chain A (also referred as α_1) is colored in cyan, and chain B (β_1) and chain D (β_2) are colored in white. The key residues are shown as a stick model, and the circles highlight the locations of identified unique interactions.

<https://doi.org/10.1371/journal.pone.0174921.g003>

$\alpha_1\beta_1$ interface changes induced by amino acid mutations

Previous structural analysis of the lowland hemoglobin variant suggested that the $\alpha_1\beta_1$ interface interaction (in particular, the interaction between α_1 Cys34 and β_1 Ser128) differs from that of the highland variant due to a mutation at β_1 Ala128 [20]. Our structural analysis revealed that the highland hemoglobin variant lacked this interaction, and also showed that the α_1 Cys34 side chain was pointed toward the subunit interface, allowing the interaction with the β_1 Pro124 main chain oxygen atom (S3 Fig).

Mutations at α_1 113, α_1 115 and α_1 116 might also affect this interface as the β_1 128 mutation. The lowland hemoglobin variant has α_1 Leu113, α_1 Ser115 and α_1 Asp116, whereas the highland hemoglobin has α_1 His113, α_1 Ala115 and α_1 Glu116. Structural analysis of the highland hemoglobin variant demonstrated that α_1 His113 and α_1 Glu116 had different coordinates among the four α subunits (Fig 3-3), resulting in different interactions with nearby residues. For example, α_1 Glu116 from chain C showed an interaction with α_1 Lys16, and chain G α_1 His113 interacted with α_1 Tyr24 and α_1 Glu116. In the lowland hemoglobin variant, these residues show no interactions with nearby residues. In addition, α_1 Trp14, which alters conformations between the deoxygenated and oxygenated states in human hemoglobin [37], seems to have a different set

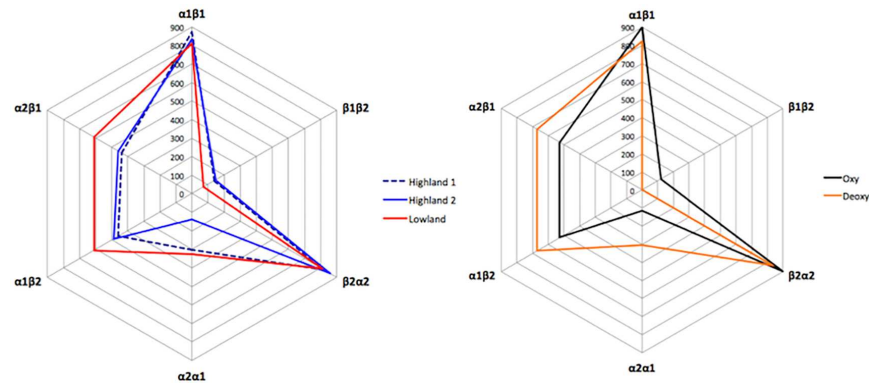


Fig 4. Difference in interface area between highland and lowland hemoglobin and human oxygenated and deoxygenated hemoglobin. Interface area of lowland hemoglobin and two highland hemoglobin tetramers were calculated by the PISA webserver. The values on the graph show the surface area in Å². The blue line is a result from one highland hemoglobin, which consists of chains A, B, C and D. The dotted dark line is a result from another highland hemoglobin (chains E, F, G and H). The lowland hemoglobin result is depicted by the red line. The intradimeric interface area of human hemoglobin was calculated using the following structures; deoxygenated structure (2DN2, orange) and oxygenated structure (2DN1, black)

<https://doi.org/10.1371/journal.pone.0174921.g004>

of interactions in deer mouse hemoglobin. In lowland hemoglobin, the α_1 Trp14 side chain was oriented toward residues α_1 113, α_1 115 and α_1 116, whereas the majority of the highland hemoglobin had an α_1 Trp14 side chain pointed toward α_1 Tyr24 (Fig 3-3). Only chain G from the highland hemoglobin had the same α_1 Trp14 coordinate as the lowland hemoglobin. Because chain G had the highest number of interactions between residues at α_1 113, α_1 115 and α_1 116, mutations at these sites can be expected to affect the packing of nearby helices in the α subunit. Such changes could account for differences in the nature of atomic contacts at the $\alpha_1\beta_1$ interface.

Discussion

The hemoglobin variants of highland and lowland deer mice are distinguished by 12 amino acid mutations. We compared structures of both variants to elucidate how these mutations account for the observed difference in hemoglobin-oxygen affinity. A previous study of the lowland hemoglobin variant revealed no atomic contact between α Trp14 and E helix residue α 67, which enhances the mobility of the E-helix (which contains the distal histidine, α His58) [20]. In the lowland hemoglobin variant, the interaction between α His50 and α Glu30 might promote tight α subunit packing as well as helix mobility [19]. In addition, the evidence suggests that the α_1 Cys34- β_1 Ser128 interaction in the lowland hemoglobin variant produced a change in the $\alpha_1\beta_1$ interface [19, 20]. Three mutations at α_1 113, α_1 115 and α_1 116 highlighted changes in nearby helix packing that stem from changes in inter-helix interactions. Additionally, α Ser71 in the highland variant interacts with α Thr68; an interaction that is not possible in the lowland variant due to the presence of α Ala71 (Fig 3-1).

The $\alpha_1\beta_2/\alpha_2\beta_1$ interfaces were different because of the main chain atom displacements between α 41 and α 54 and the stability of the α His45-heme interaction, and these were enhanced by the α His/Pro50 mutation. Additionally, the $\alpha_1\beta_1$ interface was altered, as the highland hemoglobin β_1 Ala128 substitution prevented interaction with α_1 Cys34, and this promoted an interaction between α_1 Cys34 and the β_1 Pro124 main chain oxygen atom.

In conclusion, the amino acid mutations that distinguish the highland and lowland deer mouse hemoglobin variants affect oxygen-binding affinity by altering interface interactions,

which are mainly attributable to mutations in the α subunit. The highland hemoglobin variant has a looser $\alpha_1\beta_2/\alpha_2\beta_1$ switch region than the lowland variant due to the $\alpha 50$ mutation, and the nature of atomic contacts at the $\alpha_1\beta_1$ interface is also different because of mutations at $\beta 128$, $\alpha 113$, $\alpha 115$ and $\alpha 116$. In guinea pig hemoglobin [38], the lack of a salt bridge between $\alpha\text{Thr}30$ and $\alpha\text{Pro}50$ conferred an increased flexibility. Also, the guinea pig hemoglobin has $\alpha\text{His}40$ instead of $\alpha\text{Pro}40$ (as in human hemoglobin), and the bulkiness of histidine affects the $\alpha_1\beta_2/\alpha_2\beta_1$ interface during the T \leftrightarrow R transition in quaternary structure. These results suggest that the modulation of allosteric interactions via changes in protein flexibility may represent an important mechanism in the evolutionary fine-tuning of hemoglobin-oxygen affinity.

Supporting information

S1 Fig. Pictures of highland hemoglobin crystals. (A) Schematic figure of the setting hemoglobin crystal. The highland hemoglobin drop was placed in the airtight glass vial coated with silicon. After injecting the reservoir, carbon monoxide was purged from the vial. (B) Picture of the crystallization system described in Fig 1A. (C) Type F crystals in the cryo-loop during data collection. (D) Type S crystals in a droplet. The white arrow indicates the location of the crystal used for the data collection. In C and D, white bars indicate 0.1 mm.

(TIF)

S2 Fig. The electron density map around heme in chain H. Comparisons of the $2F_o-F_c$ map around β subunit hemes between chain H (no ligand bound) and chain B (water bound shown as a red sphere). The contour level is 1.5 sigma, and bound water molecule is shown in red sphere (figure was generated by PyMOL).

(TIF)

S3 Fig. Differences in $\alpha_1\beta_1$ interface due to amino acid substitution. The highland hemoglobin α subunit is colored in cyan, and the lowland hemoglobin α subunit is colored in pink. The corresponding β subunit is colored in gray. Key residues at the $\alpha_1\beta_1$ interface are labeled, and interactions identified by the PISA webserver are depicted with black dotted lines.

(TIF)

Acknowledgments

We thank the staff of the APS beamline 14-BM-C for expert technical assistance. This work was funded by a grant from the National Institute of Health/National Heart, Lung, and Blood Institute (HL087216).

Author Contributions

Conceptualization: HM JFS TK.

Data curation: NI NM SB CN.

Formal analysis: NI NM SB CN.

Funding acquisition: HM JFS TK.

Investigation: NI NM SB CN.

Project administration: HM.

Resources: NI.

Writing – original draft: NI NM SB TK CN JFS HM.

References

1. Perutz MF. Structure of hemoglobin. Brookhaven symposia in biology. 1960; 13:165–83. PMID: [13734651](#)
2. Perutz MF. Stereochemistry of cooperative effects in haemoglobin. *Nature*. 1970; 228(5273):726–39. Epub 1970/11/21. PMID: [5528785](#)
3. Perutz MF. Nature of haem-haem interaction. *Nature*. 1972; 237(5357):495–9. PMID: [12635193](#)
4. Birukou I, Soman J, Olson JS. Blocking the gate to ligand entry in human hemoglobin. *The Journal of biological chemistry*. 2011; 286(12):10515–29. PubMed Central PMCID: PMC3060505. <https://doi.org/10.1074/jbc.M110.176271> PMID: [21193395](#)
5. Shadrina MS, English AM, Peslherbe GH. Effective simulations of gas diffusion through kinetically accessible tunnels in multisubunit proteins: O₂ pathways and escape routes in T-state deoxyhemoglobin. *Journal of the American Chemical Society*. 2012; 134(27):11177–84. <https://doi.org/10.1021/ja300903c> PMID: [22690872](#)
6. Srajer V, Ren Z, Teng TY, Schmidt M, Ursby T, Bourgeois D, et al. Protein conformational relaxation and ligand migration in myoglobin: a nanosecond to millisecond molecular movie from time-resolved Laue X-ray diffraction. *Biochemistry*. 2001; 40(46):13802–15. PMID: [11705369](#)
7. Srajer V, Royer WE Jr. Time-resolved x-ray crystallography of heme proteins. *Methods in enzymology*. 2008; 437:379–95. PubMed Central PMCID: PMC3287071. [https://doi.org/10.1016/S0076-6879\(07\)37019-5](https://doi.org/10.1016/S0076-6879(07)37019-5) PMID: [18433638](#)
8. Srajer V, Teng T, Ursby T, Pradervand C, Ren Z, Adachi S, et al. Photolysis of the carbon monoxide complex of myoglobin: nanosecond time-resolved crystallography. *Science*. 1996; 274(5293):1726–9. PMID: [8939867](#)
9. Rubin MM, Changeux JP. On the nature of allosteric transitions: implications of non-exclusive ligand binding. *Journal of molecular biology*. 1966; 21(2):265–74. PMID: [5972463](#)
10. Fischer S, Olsen KW, Nam K, Karplus M. Unsuspected pathway of the allosteric transition in hemoglobin. *Proceedings of the National Academy of Sciences of the United States of America*. 2011; 108(14):5608–13. PubMed Central PMCID: PMC3078355. <https://doi.org/10.1073/pnas.1011995108> PMID: [21415366](#)
11. Adachi S, Park SY, Tame JRH, Shiro Y, Shibayama N. Direct observation of photolysis-induced tertiary structural changes in hemoglobin. *Proceedings of the National Academy of Sciences of the United States of America*. 2003; 100(12):7039–44. <https://doi.org/10.1073/pnas.1230629100> PMID: [12773618](#)
12. Storz JF, Scott GR, Cheviron ZA. Phenotypic plasticity and genetic adaptation to high-altitude hypoxia in vertebrates. *J Exp Biol*. 2010; 213(Pt 24):4125–36. PubMed Central PMCID: PMC3062992. <https://doi.org/10.1242/jeb.048181> PMID: [21112992](#)
13. Storz JF. Hemoglobin–oxygen affinity in high-altitude vertebrates: is there evidence for an adaptive trend? *The Journal of experimental biology*. 2016; 219(20):3190–203.
14. Storz JF, Moriyama H. Mechanisms of hemoglobin adaptation to high altitude hypoxia. *High Alt Med Biol*. 2008; 9(2):148–57. Epub 2008/06/27. <https://doi.org/10.1089/ham.2007.1079> PMID: [18578646](#)
15. Jensen B, Storz JF, Fago A. Bohr effect and temperature sensitivity of hemoglobins from highland and lowland deer mice. *Comp Biochem Physiol A Mol Integr Physiol*. 2016; 195:10–4. PubMed Central PMCID: PMC4789091. <https://doi.org/10.1016/j.cbpa.2016.01.018> PMID: [26808972](#)
16. Storz JF, Runck AM, Sabatino SJ, Kelly JK, Ferrand N, Moriyama H, et al. Evolutionary and functional insights into the mechanism underlying high-altitude adaptation of deer mouse hemoglobin. *Proceedings of the National Academy of Sciences of the United States of America*. 2009; 106(34):14450–5. Epub 2009/08/12. <https://doi.org/10.1073/pnas.0905224106> PMID: [19667207](#)
17. Natarajan C, Hoffmann FG, Lanier HC, Wolf CJ, Cheviron ZA, Spangler ML, et al. Intraspecific polymorphism, interspecific divergence, and the origins of function-altering mutations in deer mouse hemoglobin. *Mol Biol Evol*. 2015; 32(4):978–97. PubMed Central PMCID: PMC34379404. <https://doi.org/10.1093/molbev/msu403> PMID: [25556236](#)
18. Storz JF, Runck AM, Moriyama H, Weber RE, Fago A. Genetic differences in hemoglobin function between highland and lowland deer mice. *J Exp Biol*. 2010; 213(Pt 15):2565–74. Epub 2010/07/20. <https://doi.org/10.1242/jeb.042598> PMID: [20639417](#)
19. Natarajan C, Inoguchi N, Weber RE, Fago A, Moriyama H, Storz JF. Epistasis among adaptive mutations in deer mouse hemoglobin. *Science*. 2013; 340(6138):1324–7. PubMed Central PMCID: PMC4409680. <https://doi.org/10.1126/science.1236862> PMID: [23766324](#)
20. Inoguchi N, Oshlo JR, Natarajan C, Weber RE, Fago A, Storz JF, et al. Deer mouse hemoglobin exhibits a lowered oxygen affinity owing to mobility of the E helix. *Acta Crystallogr Sect F Struct Biol Cryst Commun*. 2013; 69(Pt 4):393–8. PubMed Central PMCID: PMC3614163. <https://doi.org/10.1107/S1744309113005708> PMID: [23545644](#)

21. Yokoyama T, Neya S, Tsuneshige A, Yonetani T, Park SY, Tame JR. R-state haemoglobin with low oxygen affinity: crystal structures of deoxy human and carbonmonoxy horse haemoglobin bound to the effector molecule L35. *Journal of molecular biology*. 2006; 356(3):790–801. <https://doi.org/10.1016/j.jmb.2005.12.018> PMID: 16403522
22. Natarajan C, Jiang X, Fago A, Weber RE, Moriyama H, Storz JF. Expression and purification of recombinant hemoglobin in *Escherichia coli*. *PLoS One*. 2011; 6(5):e20176. PubMed Central PMCID: PMC3098879. <https://doi.org/10.1371/journal.pone.0020176> PMID: 21625463
23. Otwinowski Z, Minor W. Processing of X-ray Diffraction Data Collected in Oscillation Mode. In: Carter JCWS, R M, editor. *Methods in Enzymology* 276. 276. New York: Academic Press; 1997. p. 307–26.
24. Adams PD, Afonine PV, Bunkoczi G, Chen VB, Davis IW, Echols N, et al. PHENIX: a comprehensive Python-based system for macromolecular structure solution. *Acta Crystallogr D Biol Crystallogr*. 2010; 66(Pt 2):213–21. PubMed Central PMCID: PMCPMC2815670. <https://doi.org/10.1107/S0907444909052925> PMID: 20124702
25. Emsley P, Lohkamp B, Scott WG, Cowtan K. Features and development of Coot. *Acta Crystallogr D Biol Crystallogr*. 2010; 66(Pt 4):486–501. PubMed Central PMCID: PMCPMC2852313. <https://doi.org/10.1107/S0907444910007493> PMID: 20383002
26. Park SY, Yokoyama T, Shibayama N, Shiro Y, Tame JR. 1.25 Å resolution crystal structures of human haemoglobin in the oxy, deoxy and carbonmonoxy forms. *Journal of molecular biology*. 2006; 360(3):690–701. Epub 2006/06/13. <https://doi.org/10.1016/j.jmb.2006.05.036> PMID: 16765986
27. Wishner BC, Ward KB, Lattman EE, Love WE. Crystal structure of sickle-cell deoxyhemoglobin at 5 Å resolution. *Journal of molecular biology*. 1975; 98(1):179–94. Epub 1975/10/15. PMID: 1195378
28. Kabsch W. A solution for the best rotation to relate two sets of vectors. *Acta Crystallographica Section A*. 1976; 32:922–3.
29. Joosten RP, te Beek TA, Krieger E, Hekkelman ML, Hooft RW, Schneider R, et al. A series of PDB related databases for everyday needs. *Nucleic Acids Res*. 2011; 39(Database issue):D411–9. PubMed Central PMCID: PMCPMC3013697. <https://doi.org/10.1093/nar/gkq1105> PMID: 21071423
30. Kabsch W, Sander C. Dictionary of protein secondary structure: pattern recognition of hydrogen-bonded and geometrical features. *Biopolymers*. 1983; 22(12):2577–637. <https://doi.org/10.1002/bip.360221211> PMID: 6667333
31. Aranda Rt, Cai H, Worley CE, Levin EJ, Li R, Olson JS, et al. Structural analysis of fish versus mammalian hemoglobins: effect of the heme pocket environment on autooxidation and heme loss. *Proteins*. 2009; 75(1):217–30. PubMed Central PMCID: PMCPMC2649966. <https://doi.org/10.1002/prot.22236> PMID: 18831041
32. Voet D, Voet JG. *Biochemistry*. 4th ed. Hoboken, NJ: John Wiley & Sons; 2011. xxv, 1428, 1–53 p. p.
33. Baldwin J, Chothia C. Haemoglobin: the structural changes related to ligand binding and its allosteric mechanism. *Journal of molecular biology*. 1979; 129(2):175–220. PMID: 39173
34. Krissinel E, Henrick K. Inference of macromolecular assemblies from crystalline state. *Journal of molecular biology*. 2007; 372(3):774–97. <https://doi.org/10.1016/j.jmb.2007.05.022> PMID: 17681537
35. Viappiani C, Abbruzzetti S, Ronda L, Bettati S, Henry ER, Mozzarelli A, et al. Experimental basis for a new allosteric model for multisubunit proteins. *Proceedings of the National Academy of Sciences of the United States of America*. 2014; 111(35):12758–63. PubMed Central PMCID: PMCPMC4156698. <https://doi.org/10.1073/pnas.1413566111> PMID: 25139985
36. Di Cera E, Robert CH, Gill SJ. Allosteric interpretation of the oxygen-binding reaction of human hemoglobin tetramers. *Biochemistry*. 1987; 26(13):4003–8. PMID: 3651431
37. Balakrishnan G, Tsai CH, Wu Q, Case MA, Pevsner A, McLendon GL, et al. Hemoglobin site-mutants reveal dynamical role of interhelical H-bonds in the allosteric pathway: time-resolved UV resonance Raman evidence for intra-dimer coupling. *Journal of molecular biology*. 2004; 340(4):857–68. <https://doi.org/10.1016/j.jmb.2004.05.013> PMID: 15223326
38. Pairet B, Jaenicke E. Structure of the altitude adapted hemoglobin of guinea pig in the R2-state. *PLoS one*. 2010; 5(8):e12389. PubMed Central PMCID: PMCPMC2927554. <https://doi.org/10.1371/journal.pone.0012389> PMID: 20811494